The Journal of the Korean Society of
Coastal and Ocean Engineers
Vol. 2, No. 4, pp. 190-199, December 1990

Determination of Vertical Mode in a Three-layered Open Sea
三層構造 外海域에서의 吹送流 鉛直모드 決定技法

Kyung Tae Jung*, Jae Youll Jin*, Jae Kwi So* and John Noye**
鄭景太*・陳在律*・蘇在貴*・존 노이**

Abstract □ The solution for wind drift current in a three-layered open sea region is derived using the Galerkin-Eigenfunction method. The presence of discontinuities in the vertical eddy viscosity required a definition of a scalar product which involves the summation of integrals defined over each layer. The expansion of fourth-order *B*-spline functions is used in determining eigenvalues and corresponding eigenfunctions. In a three-layered system a low value of eddy viscosity is prescribed within the pycnocline to represent the suppression of turburent intensity at the thermocline level. A high concentration of knots within the pycnocline is important in determining eigenfunctions and the associated eigenvalues accurately. Due to the global property of eigenfunctions nonphysical oscillations appear in the current profiles below the surface layer, particularly within the pycnocline.

要 旨: 3層 構造를 갖는 大陸棚 外海域에서의 吹送流 豫測을 위한 Galerkin 解를 Eigenfunction 展開를 통해 誘導하였다. 水深變化를 결정짓는 鉛直亂流擴散 係數가 層間에 不連續的으로 變化토록 定義되므로 內積分 定義時 層別積分이 등장한다. Eigenfunction 및 Eigenvalue 算出을 위해 B-spline 函數展開가 이용되는데 정확한 계산을 위해서는 亂流活動이 극도로 低下되는 Pycnocline 내에 많은 Knot들을 配定함이 필요한 것으로 나타났다. 비록 Eigenfunction이 層間에 급격한 변화를 가지나 여전히 海水表面부터 海底面間의 전 구간에 걸쳐 定義되는 連續函數이므로 Gibbs 効果에 따른 解의 振動現象이 表層下, 특히 Pycnocline 내에서 出現하였다.

1. INTRODUCTION

The solution of the three-dimensional hydrodynamic equations describing wind induced flows in a layered sea has been developed in recent years using the Galerkin-Eigenfunction method in the vertical (Heaps (1983), Heaps and Jones (1983), Jung and Noye (1988)). In the layered system modeled in all this work internal discontinuities are present in the prescribed eddy viscosity profile, and consequently a *layered* eigenvalue problem is posed. The eigenfunctions are defined continuously throughout the depth but, due to the jump in values of density and eddy viscosity at the interfaces, their first derivatives are discontinuous.

The layered eigenvalue problem can be solved by either analytic or numerical methods. In the analytic approach (Heaps (1983), Heaps and Jones (1983)) eigenvalues and eigenfunctions are determined through a mode matching technique, but its use is restricted to a simple functional form of eddy viscosty. To handle arbitrary variation of eddy viscosity in a flexible manner, Jung and Noye (1988) devised a numerical method of solving the two-layered Sturm-Liouville boundary value problem with a strong discontinuity in the coefficient of the second-order differential operator. The Galerkin method with expansion of fourth-order B-spline functions are used to approximate the basis set of eigenfunctions along with the use of a scalar product which involves the sum-

*韓國海洋研究所 沿岸工學研究室(Coastal Engineering Laboratory, Korea Ocean Research and Development Institute, Ansan P. O. Box 29, Seoul 425-600, Korea)
**Department of Applied Mathematics, The University of Adelaide, G.P.O. Box 498, Adelaide, South Australia.

mation of integrals defined over each layer.

In this paper Jung and Noye's method is extended to the three-layered system which consists of the surface layer, the pycnocline and the bottom layer. There have been extensive numerical experiments conducted by Davies (1985a, b, 1986) and Davies and Furnes (1986) which have led to a description of the overall features of wind induced motion in both homogeneous and stratified seas. Our discussion is therefore centered on the accuracy of the method in computing the eigenfunctions and the current profiles through the depth. Following Davies (1983) and Furnes (1983), the limit conditions for the eigenfunctions and eigenvalues are introduced in a generalised separable form. Results from this study will serve as a basis for realistic applications in the future.

2. HYDRODYNAMIC EQUATIONS FOR THE THREE-LAYERED SYSTEM

The linear equations of motion in sigma coordinates which govern the drift current in a three-layered open sea are given by,

$$\frac{\partial U_j}{\partial t} - \gamma V_j = \frac{\partial}{H^2 \partial \sigma}\left[N_j \frac{\partial U_j}{\partial \sigma}\right], \tag{1}$$

$$\frac{\partial V_j}{\partial t} + \gamma U_j = \frac{\partial}{H^2 \partial \sigma}\left[N_j \frac{\partial V_j}{\partial \sigma}\right] \tag{2}$$

with $j = 1, 2, 3$ and $\sigma = -z/H$.

In the above equations, t denotes time; x, y, z are the Cartesian spatial coordinates, with z the depth below the undisturbed surface which contains the x and y axes. Also U_j and V_j are horizontal components of currents in the x, y directions, respectively; N_j are vertical eddy viscosity coefficient, with the subscripts j denoting values at the jth layer; H is the depth of the sea floor below the undisturbed surface level and g is the acceleration due to gravity; and γ is the Coriolis parameter given by $\gamma = 2\omega_e \sin \phi_e$ where ω_e is the circular frequency of the earth's rotation and ϕ_e is the latitude which is considered positive in the Northern Hemisphere and negative in the Southern Hemisphere.

In order to solve the system of equations (1) and (2) for U_j, V_j, $j = 1,2,3$ boundary conditions have to be given at the sea surface and at the sea bed, together with interfacial conditions. Surface boundary conditions at $\sigma = \xi_0 = 0$ are

$$-\frac{\rho_1}{H}\left[N_1 \frac{\partial U_1}{\partial \sigma}\right] = \tau_{sx}, \quad -\frac{\rho_1}{H}\left[N_1 \frac{\partial V_1}{\partial \sigma}\right] = \tau_{sy}, \tag{3}$$

where τ_{sx} and τ_{sy} denote the components of surface wind stress. For tidal flow the surface stress goes to zero.

At the sea bed, $\sigma = \xi_3 = 1$, a bottom stress condition of the form

$$-\frac{\rho_3}{H}\left[N_3 \frac{\partial U_3}{\partial \sigma}\right] = \tau_{bx}, \quad -\frac{\rho_3}{H}\left[N_3 \frac{\partial V_3}{\partial \sigma}\right] = \tau_{by}, \tag{4}$$

is applied, where τ_{bx} and τ_{by} denote the x and y components of bottom stress. In a linear model it is appropriate to use a linear formulation of bottom stress, thus

$$\tau_{bx} = \rho_3 K_b U_b, \quad \tau_{by} = \rho_3 K_b V_b \tag{5}$$

where K_b is a constant coefficient of friction and U_b, V_b are the components of current at the sea bed.

Conditions of continuity of velocity and stress at the undisturbed level of interface, $\sigma = \xi_j$, are given by,

$$U_j = U_{j+1}, \qquad V_j = V_{j+1}, \tag{6}$$

$$\rho_j \left[N_j \frac{\partial U_j}{\partial \sigma}\right] = \rho_{j+1}\left[N_{j+1} \frac{\partial U_{j+1}}{\partial \sigma}\right], \tag{7}$$

$$\rho_j \left[N_j \frac{\partial V_j}{\partial \sigma}\right] = \rho_{j+1}\left[N_{j+1} \frac{\partial V_{j+1}}{\partial \sigma}\right]. \tag{8}$$

3. GALERKIN SOLUTIONS USING THE EXPANSION OF EIGENFUNCTIONS OVER THE VERTICAL SPACE

In the three-layered system the scalar product is defined in summation of integrals over each layer, namely,

$$\langle \phi_j, \psi_j \rangle = \sum_{j=1}^{3} \int_{\xi_{j-1}}^{\xi_j} \phi_j \cdot \psi_j \, d\sigma \tag{9}$$

where ϕ_j and ψ_j represent a pair of square integrable functions defined at the jth layer. It is assumed that the vertical variation of eddy viscosity is fixed, having a functional form denoted by $\mu(\sigma)$, that is,

$$N_j(t, \sigma) = \alpha(t) \cdot \mu_j(\sigma) \quad \text{for } \xi_{j-1} \leqq \sigma \leqq \xi_j. \tag{10}$$

For this variation of eddy viscosity time-invariant eigenfunctions and eigenvalues can be determined. Solutions are sought with respect to the scalar product (9) using the eigenfunctions defined through the depth as follows:

$$f = f_j \quad \text{for } \xi_{j-1} \leqq \sigma \leqq \xi_j. \tag{11}$$

The r th eigenfunction at the jth layer is denoted in the local form:

$$f_r = f_{j,r} \quad \text{for } \xi_{j-1} \leqq \sigma \leqq \xi_j. \tag{12}$$

Expanding the two horizontal components of current in terms of m eigenfunctions $f_{j,r}$ and coefficients $A_r(t)$ and $B_r(t)$ give,

$$U_j(\sigma, t) = \sum_{r=1}^{m} A_r(t) f_{j,r}(\sigma),$$

$$V_j(\sigma, t) = \sum_{r=1}^{m} B_r(t) f_{j,r}(\sigma)$$

$$\text{for } \xi_{j-1} \leqq \sigma \leqq \xi_j. \tag{13}$$

Let λ_k and f_k, $k = 1, \ldots, m$ be a set of eigenvalues and eigenfunctions determined from

$$\frac{d}{d\sigma}\left[\mu_j \frac{df_j}{d\sigma}\right] = -\lambda f_j, \quad j = 1, 2, 3 \tag{14}$$

subject to separable limit conditions

$$\left[\mu_1 \frac{df_1}{d\sigma}\right] = \beta_1 f_1 \quad \text{at } \sigma = 0, \tag{15}$$

$$\left[\mu_3 \frac{df_3}{d\sigma}\right] = \beta_2 f_3 \quad \text{at } \sigma = 1, \tag{16}$$

and interfacial conditions

$$f_j = f_{j+1}, \tag{17}$$

$$\mu_j \left[\frac{df_j}{d\sigma}\right] = \mu_{j+1}\left[\frac{df_{j+1}}{d\sigma}\right]\left[\frac{\rho_{j+1}}{\rho_j}\right]. \tag{18}$$

Applying the Galerkin method to (1) (see Jung (1989) for details) and using the orthogonal property of eigenfunctions, namely,

$$\langle f_{j,r}, f_{j,k} \rangle = \sum_{j=1}^{3} \frac{\rho_j}{\rho_1} \int_{\xi_{j-1}}^{\xi_j} f_{j,r} \cdot f_{j,k} \, d\sigma = 0$$

$$\text{for } r \neq k \tag{19}$$

we obtain

$$\frac{\partial A_k}{\partial t} = \gamma B_k - \frac{\alpha}{H^2}\lambda_k A_k + (J_{x,k} + K_{x,k})\Phi_k$$

where

$$J_{x,k} = \frac{\tau_{sx}}{\rho_1 H} f_k(0) - \frac{\tau_{bx}}{\rho_1 H} f_k(1), \tag{21}$$

$$K_{x,k} = \frac{\alpha}{H^2} \sum_{r=1}^{m} A_r \left[\beta_1 f_k(0) f_r(0) - \left[\frac{\rho_3}{\rho_1}\right]\beta_2 f_k(1) f_r(1)\right], \tag{22}$$

$$\Phi_k = \langle f_{j,k}, f_{j,k} \rangle^{-1}, \quad k = 1, 2, 3. \tag{23}$$

Similarly,

$$\frac{\partial B_k}{\partial t} = -\gamma A_k - \frac{\alpha}{H^2}\lambda_k B_k + [J_{y,k} + K_{y,k}]\Phi_k \tag{24}$$

where

$$J_{y,k} = \frac{\tau_{sy}}{\rho_1 H} f_k(0) - \frac{\tau_{by}}{\rho_1 H} f_k(1), \tag{25}$$

$$K_{y,k} = \frac{\alpha}{H^2} \sum_{r=1}^{m} B_r \left[\beta_1 f_k(0) f_r(0) - \left[\frac{\rho_3}{\rho_1}\right]\beta_2 f_k(1) f_r(1)\right], \quad k = 1, 2, 3. \tag{26}$$

The vertical modes in (20) and (24) are coupled through the terms for the bottom friction $J_{x,k}$m $J_{y,k}$ and the stressing terms $K_{x,k}$, $K_{y,k}$ which involve β_1 and β_2. A matrix inversion is required to solve for the coefficients of the eigenfunction expansion. With $K_b = 0$, the system of equations becomes uncoupled.

Consider the alternative expansion of the U_i and V_i velocities used in a series of works by Heaps,

namely,

$$U_j(\sigma, t) = \sum_{r=1}^{m} A_r(t)\,\Phi_r f_{j,r}(\sigma) \quad \text{for } \xi_{j-1} \leqq \sigma \leqq \xi_j, \tag{27}$$

$$V_j(\sigma, t) = \sum_{r=1}^{m} B_r(t)\,\Phi_r f_{j,r}(\sigma) \quad \text{for } \xi_{j-1} \leqq \sigma \leqq \xi_j \tag{28}$$

With the use of relations

$$A_r \rightarrow \hat{A}_r \Phi_r, \quad B_r \rightarrow \hat{B}_r \Phi_r, \tag{29}$$

(20) and (24) reduce to

$$\frac{\partial \hat{A}_k}{\partial t} = \gamma \hat{B}_k - \frac{\alpha}{H^2}\lambda_k \hat{A}_k + (\hat{J}_{x,k} + \hat{K}_{x,k}), \tag{30}$$

$$\frac{\partial \hat{B}_k}{\partial t} = -\gamma \hat{A}_k - \frac{\alpha}{H^2}\lambda_k \hat{B}_k + (\hat{J}_{y,k} + \hat{K}_{y,k}), \tag{31}$$

where

$$J_{x,k} = \frac{\hat{\tau}_{sx}}{\rho_1 H} f_k(0) - \frac{\hat{\tau}_{bx}}{\rho_1 H} f_k(1), \tag{32}$$

$$J_{y,k} = \frac{\hat{\tau}_{sy}}{\rho_1 H} f_k(0) - \frac{\hat{\tau}_{by}}{\rho_1 H} f_k(1), \tag{33}$$

$$\hat{K}_{x,k} = \frac{\alpha}{H^2} \sum_{r=1}^{m} \hat{A}_r \Phi_r [\beta_1 f_k(0) f_r(0) - (\frac{\rho_3}{\rho_1}) \beta_2 f_k(1) f_r(1)], \tag{34}$$

$$\hat{K}_{y,k} = \frac{\alpha}{H^2} \sum_{r=1}^{m} \hat{B}_r \Phi_r [\beta_1 f_k(0) f_r(0) - (\frac{\rho_3}{\rho_1}) \beta_2 f_k(1) f_r(1)] \tag{35}$$

$$\hat{\tau}_{b\,x} = \rho_3 K_b \sum_{r=1}^{m} \hat{A}_r \Phi_r f_r(1), \tag{36}$$

$$\hat{\tau}_{b\,y} = \rho_3 K_b \sum_{r=1}^{m} \hat{B}_r \Phi_r f_r(1), \quad k = 1, 2, 3. \tag{37}$$

4. NUMERICAL DETERMINATION OF EIGENFUNCTIONS AND EIGENVALUES

To handle arbitrary variation of the vertical eddy viscosity in a flexible manner, it is necessary to use a numerical method of solving the layered eigenvalue problem. Taking the scalar product (9) of (14) with $f_{j,k}$ intergrating by parts, using limit conditions (21) to (23), yields

$$<\mu_j \frac{df_{i,r}}{d\sigma}, \frac{df_{i,k}}{d\sigma}> = -\beta_1 + \beta_2 (\frac{\rho_3}{\rho_1}) f_r(1)\, f_k(1) + \lambda <f_{i,r}, f_{j,k}> \quad k = 1, 2, 3. \tag{38}$$

Following Davies (1981) and Jung and Noye (1988), the r th eigenfunction is represented in terms of a set of fourth-order B-spline functions M_l, $l = 1, \ldots, n$, namely,

$$f_{j,q}(\sigma) = \sum_{l=1}^{n} L_{l,q} \cdot M_l(\sigma) \quad \text{for } \xi_{j-1} \leqq \sigma \leqq \xi_j \tag{39}$$

where j = 1, 2, 3 and q = 1, ..., m.

Substitution of the B-spline expansion (39) into equation (38) yields the matrix equation

$$[L]_T [\bar{D}] [L] = [Q] [L]^T [C] [L]. \tag{40}$$

In this equation: [L] is an $n \times n$ matrix with (r, k) the element

$$L_{r,k}; \tag{41}$$

$[L]^T$ is its transpose; [Q] is a matrix of eigenvalues, that is, with (r, k)th elements

$$Q_{r,k} = \lambda_k \quad \text{if } r = k, \quad Q_{r,k} = 0 \quad \text{if } r \neq k; \tag{42}$$

$[\bar{D}] = [D + B]$ and $[D]$ is a $n \times n$ matrix with (r, k)th elements

$$\sum_{j=1}^{3} \frac{\rho_3}{\rho_1} \int_{\xi_{j-1}}^{\xi_j} \mu_j \frac{dM_r}{d\sigma} \frac{dM_k}{d\sigma}\, d\sigma; \tag{43}$$

[B] is a $n \times n$ matrix with (r, k) th elements

$$\beta_1 - \beta_2 (\frac{\rho_3}{\rho_1}) f_r(1) f_k(1); \tag{44}$$

and [C] is a $n \times n$ matrix with (r,k) th element

$$\sum_{j=1}^{3} \frac{\rho_3}{\rho_1} \int_{\xi_{j-1}}^{\xi_j} M_r M_k d\sigma. \tag{45}$$

The matrices [C] and [$\bar{D}$] are sparse because the B-splines have restricted support. Once the coefficients $L_{r,k}$ are defined from (40), the eigenfunctions are correspondingly defined by (39). An alternative to using the Galerkin method with an expansion of B-splines is using an iterative method described by Furnes (1983), which may be advantageous over the Galerkin method when the accuracy of the computed eigenvalues and eigenfunctions has to be monitored (Davies and furnes (1986)). It is apparent that use of the Runge-Kutta-Merson method will be more effective if initial estimates of eigenvalues are made by the Galerkin method.

5. THE ACCURACY OF NUMERICALLY DETERMINED EIGENFUNCTIONS

Fig. 1 shows a schematic variation of density and eddy viscosity considered in this study. The continuous variation of density is approximated in terms of three homogeneous layers consisting of the surface layer, the transition layer, known as the pycnocline, and the bottom layer. Although the models described in Section 2 allow for an arbitrary variation of eddy viscosity within each layer, in the interest of examining the accuracy of the method the depth variation of eddy viscosity sketched in Fig. 1 (b) is used in most of computations. To denote values in the surface, transition and bottom layers suffices T, P, B are used.

In order to examine the accuracy of numerically determined eigenfunctions calculations are performed for a three-layered eddy viscosity profile with $N_T = 300$, $N_P = 10$, $N_B = 100 cm^2 s^{-1}$, $\Delta_T = 25$, $\Delta_P = 15$, $\Delta_B = 60$ m and various distributions of knots (Table 1). The distributions K1 and K3 are composed of 33 and 50 quasi-uniform interior knots through the vertical, respectively, and the distributions K2, K4 and K5 are composed of 33, 50 and 67 non-uniform interior knot spacings with concentration of knots near the interfaces and within the pycnocline (the number of interior knot spacings is given by $\bar{m} = m - 3$). The exact values of λ_k and Φ_k were computed iteratively from the transcendental equation derived analytically (see Jung (1989)).

It is apparent from Table 1 that increasing the number of B-spline functions gives an improved accuracy in numerically determined eigenvalues and eigenfunctions. It has been revealed in a series of preliminary computations that for a given number of B-spline functions a high concentration of knots within the pycnocline, particularly at the proximity of the upper surface of the pycnocline, is important

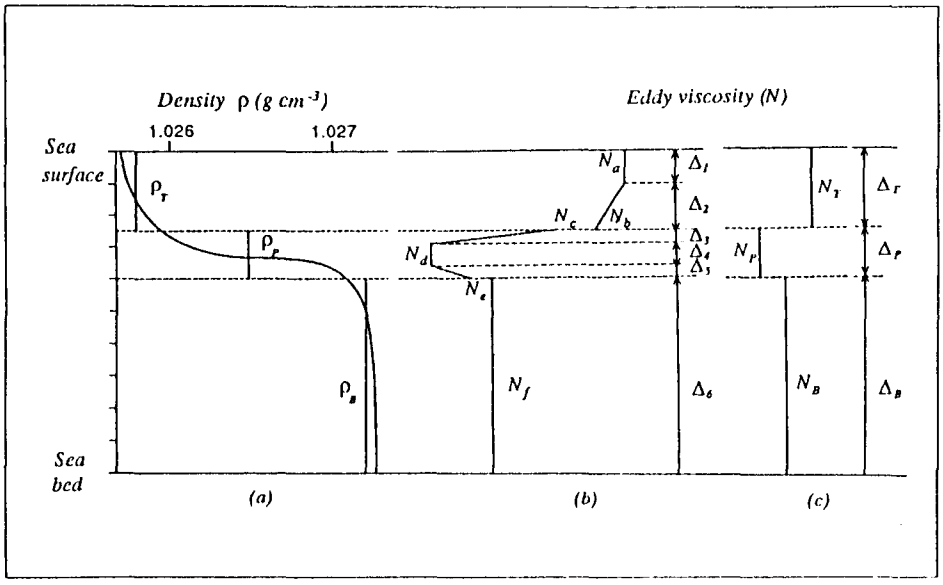

Fig. 1 A schematic variation of density and eddy viscosity through the vertical.

Table 1. Eigenvalues computed using a three-layered eddy viscosity distribution shown in Fig. 1(c), with $\Delta_T = 25$, $\Delta_P = 15$, $\Delta_B = 60$ m, $N_T = 300$, $N_P = 10$ and $N_T = 100$ cm^{2}s^{-1}, with a no-slip condition for a range of knot distributions

Distribution $\overline{m}$ =	K1 33	K2 33	K3 50	K4 50	K5 67	Exact
r = 1	1.076	1.011	1.052	1.008	1.008	1.008
2	6.639	6.359	6.523	6.349	6.349	6.345
3	34.116	30.041	32.613	29.893	29.892	29.819
4	57.120	51.649	54.447	51.542	51.541	51.482
5	117.117	109.123	114.605	108.737	108.734	108.538
10	478.733	415.227	429.679	412.568	412.563	412.389
15	1407.633	1180.577	1138.278	1079.181	1078.798	1076.924
20	2971.537	2283.083	2189.600	1819.600	1817.356	1816.038
25	5174.325	7386.768	3612.439	3045.295	3013.736	3003.123
30	8012.397	30799.402	6044.786	4350.115	4247.103	4228.482
35			9220.318	6478.395	5700.169	5699.498
40			13465.445	11119.358	7907.935	7645.858

in determining eigenfunctions and the associated eigenvalues accurately. When knot spacings are not compressed near the interfaces, wiggles appear in the numerically computed eigenfunctions particularly near the bottom of the surface layer. If an insufficient number of B-splines are used along with a uniform distribution of knots, regions of high shear (near the upper and lower surfaces of the pycnocline) are smoothed out. If the knots of B-spline functions are excessively concentrated within certain regions without increasing the total number of knots involved in the calculation, the accuracy of higher eigenvalues and eigenfunctions is rapidly decreased. In order to accurately compute up to thirty eigenfunctions, distribution K5 has been required. In this study about 67 interior knot spacings, with a distribution similar to K5 have been used.

6. FORM OF VERTICAL MODES

Fig. 2 displays the first five vertical modes evaluated numerically with m = 67 and 24, and with a no-slip bottom boundary condition, $\beta_2 = \infty$, and two linear slip bottom boundary conditions with $\beta_2 = 0$, $\beta_2 = -K_bH/\alpha$, for a range of eddy viscosity profiles. The forms of vertical modes are primarily affected by the vertical dependence of the coefficient

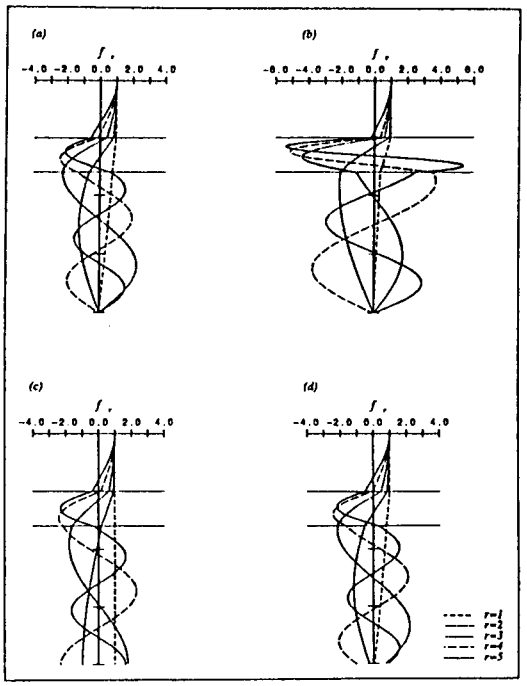

Fig. 2 The first five vertical modes of the three-layered system, obtained using the profile Fig. 1(c), computed with: $\Delta_T = 25$, $\Delta_P = 15$, $\Delta_B = 60$ m; $N_T = 300$, $N_B = 100$ cm^{2}s^{-1}; $\rho_T = 1025.8$, $\rho_P = 1026.5$, $\rho_B = 1027.2$ g cm^{-3}; $_1 = 0$; and (a) $N_P = 50$ cm^{2}s^{-1} with $\beta_2 = \infty$; (b) N_P cm^{2}s^{-1} with $\beta_2 = \infty$: (c) $N_P = 50$ cm^{2}s^{-1} with $\beta_2 = 0$; (d) $N_P = 50$, $\alpha = 142.5$ cm^{2}s^{-1} with $\alpha\beta_2 - K_BH = -0.2$ cm^{2}s^{-1}.

of the second-order viscosity operator and by limit conditions used. Note that the domain-averaged value of eddy viscosity, α is not involved in determining the structure of vertical modes. The role of density on the determination of vertical modes is negligibly small because $\Delta\rho/\rho = O(10^{-3})$. With a very low value of N_P the eigenfunctions show regions of rapid shear at the upper and lower surfaces of the pycnocline. This is due to the requirement $\rho_j \mu_j \partial f_j/\partial\sigma = \rho_{j+1}\mu_{j+1}\partial f_{j+1}/\partial\sigma$ at each of the interfaces.

As a property of eigenfunctions, the rth vertical mode has r-1 zero in the open interval (0, 1) for both the slip and no-slip boundary conditions. The zeros of the rth eigenfunction are placed between two consecutive zeros of the (r-1)th eigenfunction. In regions in whcih values of eddy viscosity are markedly reduced, zeros are concentrated with respect to the rest of the water column. This leads to a rapid change of the modal structure within the pycnocline.

An important feature is that, as a consequence of the homogeneous limit conditions, the first eigenvalue is $\lambda_1 = 0$ and the corresponding eigenfunction is $f_1(\sigma) = 1$. It should be noted that local variations of eddy viscosity and density jump have no influence on the first mode. With any other combination of limit conditions at the domain boundary, for example when a no-slip or stressing condition is enforced at the sea bed, the first vertical mode is no longer independent of vertical eddy viscosity and density.

Fig. 3 and Table 2 show how sensitive the modal structure is to changes in the value of N_P and their functional form within the pycnocline. It is evident that as N_P is increased, while keeping N_T and N_B constant, the region of high shear within the pycnocline is significantly reduced. Particularly, for the two la-

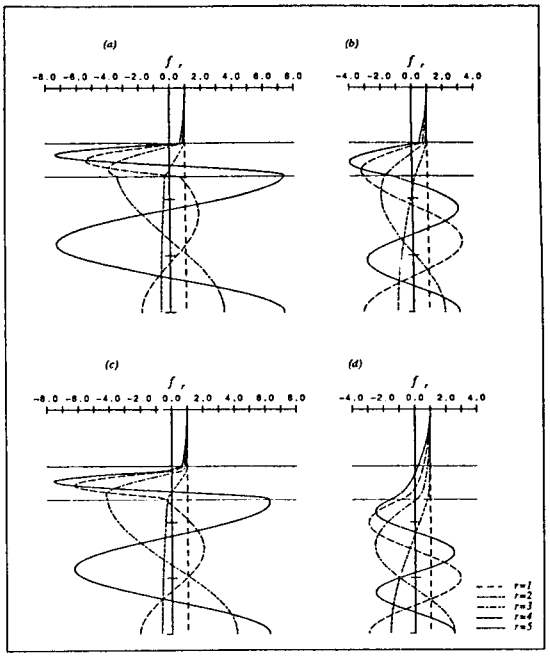

Fig. 3. The first five vertical modes of the three-layered system, obtained using the profile in fig. 1 (c), computed with: $\rho_T = 1025.8$, $\rho_P = 1026.5$, $\rho_B = 1027.2$g cm^{-3}; $\beta_1 = \beta_2 = 0$; and (a) $\Delta_T = 25$, $\Delta_P = 15$, $\Delta_B = 60$ m; $N_T = 1000$, $N_P = 10$, $N_B = 100$ cm^{2}s^{-1}; (b) $\Delta_T = 25$, $\Delta_P = 15$, $\Delta_B = 60$ m; $N_T = 1000$, $N_P = 50$, $N_B = 100$ cm^{2}s^{-1}; (c) $\Delta_1 = 22.5$, $\Delta_2 = 2.5$, $\Delta_3 = 2.5$, $\Delta_4 = 10$, $\Delta_5 = 2.5$, $\Delta_6 = 60$ m; $N_a = 1000$, $N_b = N_c = 100$, $N_d = 10$, $N_e = N_f = 100$ cm^{2}s^{-1}; (d) $\Delta_T = 25$, $\Delta_P = 15$, $\Delta_B = 60$ m; $N_T = 1000$, $N_B = 100$ cm^{2}s^{-1}, and a linear decrease within the pycnocline with $N_b = N_c = N_T$, $N_e = N_B$.

Table 2. Values of λ_k and Φ_k for the first seven vertical modes computed for the three-layered eddy viscosity distribution (a), (b), (c) and (d) in Fig. 2.

	(a)		(b)		(c)		(d)	
	λ_r	Φ_r	λ_r	Φ_r	λ_r	Φ_r	λ_r	Φ_r
$r=1$	0.000	0.999	0.000	0.999	0.000	0.999	0.000	0.999
2	0.953	2.233	1.169	2.159	1.204	2.139	3.141	1.049
3	7.810	0.207	9.011	0.162	9.019	0.153	15.945	0.450
4	16.747	0.294	22.468	0.276	23.678	0.260	40.366	0.343
5	34.747	0.049	40.016	0.058	40.611	0.063	75.584	0.453
6	56.795	0.123	74.497	0.097	77.038	0.075	118.311	0.889
7	81.167	0.032	96.846	0.075	100.843	0.110	163.117	1.388

yered eddy viscosity profile (with $N_P > N_B$) the first five vertical modes show no shear in the transitional layer and their derivatives in the vertical no longer change sign there (Fig. 3 (d)). When the values of piecewise eddy viscosity are joined in a piecewise-linear manner in the vicinity of interface levels, the higher vertical modes tend to show a smooth variation at the interface (Fig. 3(c)).

Comparing Fig. 3(a) with (c), it is evident that with a small correction to the eddy viscosity profile across the upper surface of the pycnocline ($\Delta_2 = \Delta_3 = 2.5$ m) the modal structure was not significantly different from that of a step-like variation of eddy viscosity, although there is some evidence that higher modes $r \geq 3$ are affected.

7. CONVERGENCE OF EIGENFUNCTION EXPANSION

To examine the structure of current profiles reproduced by the expansion of eigenfunctions, steady state and time dependent responses of an unbounded sea subject to the impulsive onset of wind stress are computed using a point model.

For steady state calculations the U and V solutions are reformulated in complex form and resulting modal equations are then inverted. As discussed by Davies (1985b, 1986) and Jung and Noye (1989), current profiles in stratified conditions are characterised by the presence of high shear within the pycnocline particularly in the proximity of the surface layer. It is evidnt from Fig. 4 that, as a consequence of the Gibbs phenomenon, nonphysical oscillations appear in the U component of the current profile in which wind stress is applied. We note that the discontinuity of the eigenfunctions itself is not a source of the Gibbs overshoots.

When N_B is increased from 50 to 1000 $cm^2 s^{-1}$, the oscillations are significantly reduced except within the pycnocline. Increasing m from 10 to 20 is not much helpful in suppressing the oscillations. A large number of eigenfunctions have to be used to smooth out the oscillations unless a cosmetic filter is applied.

The time dependent numerical solution of (30) and (31) are generated from quiescent state of motion

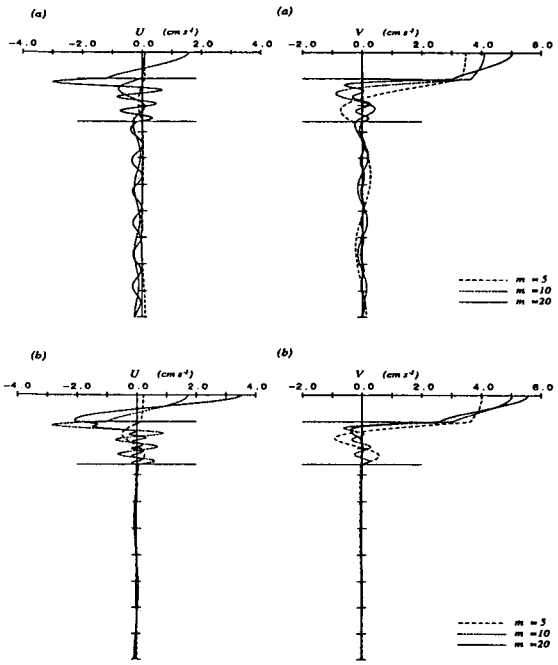

Fig. 4. Steady velocity profiles of the U and V components of wind drift current, obtained using the profile in Fig. 1(c), in a three-layered system computed using a basis set of eigenfunctions, with: $\Delta_T = 25$, $\Delta_P = 40$, $\Delta_B = 185$ m; $N_T = 150$, $N_P = 10$ $cm^2 s^{-1}$; $k_b = 0.2$ cm s^{-1}; $\rho_T = 1025.8$, $\rho_P = 1026.5$, $\rho_B = 1027.2$ $g\ cm^{-3}$; $\beta_1 = \beta_2 = 0$; and (a) $N_B = 50$ $cm^2 s^{-1}$; (b) $N_B = 1000$ $cm^2 s^{-1}$.

described by a zero initial velocity field. The surface wind stress 1 dyne cm^2 is suddenly applied at $t = 0$. Calculations are performed on a staggered finite difference grid with periodic boundary conditions. Once again we note the presence of nonphysical oscillations in the computed current profiles, particularly within the pycnocline (Fig. 5). As seen in the steady state computation, current profiles in the bottom layer are almost free of oscillations when $N_B \equiv 1000$ $cm^2 s^{-1}$ is used. However, in a series of preliminary computations it has been found that, despite the slow convergence near the sea surface and the Gibbs overshoots particularly within the pycnocline, the layer-mean values of current were computed accurately even with only five vertical modes.

In regions where strong tidal currents are omnipresent, it is necessary to increase the vertical variation of the eddy viscosity at the bottom layer to a

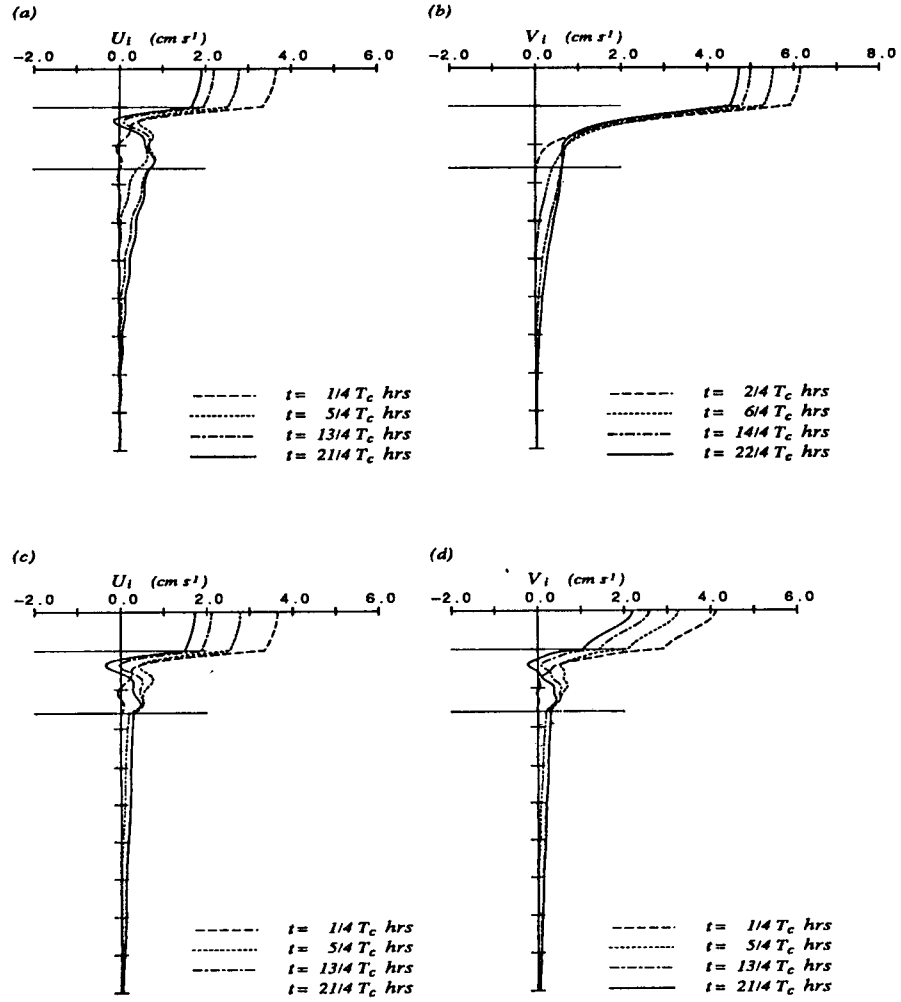

Fig. 5. Velocity profiles of U and V components of wind drift current, obtained using the profile in Fig. 1 (c), at various time steps computed using a basis set of eigenfunctions, with: $\Delta_T = 25$, $\Delta_P = 40$, $\Delta_B = 185$ m; $N_T = 1000$, $N_P = 10$ m^2s^{-1}; $\rho_T = 1025.8$, $\rho_P = 1026.5$, $\rho_B = 1027.2$g cm^{-3}; $k_b = 0.2$ cm s^{-1}; $\beta_1 = \beta_2 = 0$; and (a), (b) $N_B = 100$ cm^2s^{-1} with m= 10; (d) $N_B = 1000$ cm^2s^{-1} with m = 20.

value comparable to that at the surface layer. Heaps and Jones (1985) have chosen values $N_T = 300$ cm^2s^{-1} and $N_B = 1000$ cm^2s^{-1} in applying a three-layered spectral model to a shelf with a depth ranging in the cross-shelf direction from 50 to 300 m. Although it was not explicitly mentioned in their paper, it is conceivable that the reason behind this choice of eddy viscosity was to take into account the tidally-induced background turbulence and at the same time to suppress the Gibbs overshoots.

8. CONCLUSION

In a three-layered system eigenfunctions oscillate very rapidly within the pycnocline where a low value of eddy viscosity is prescribed to represent the reduced turbulent intensity. Concentrating the knots of B-spline functions across the interfaces is also of importance in reproducing the rapid variation of eigenfunctions within the pycnocline.

The rate of convergence of the spectral method

depends upon whether nonphysical oscillations arises as a consequence of the Gibbs phenomenon. It is known that classical continuous functions such as trigonometric functions, Chebyshev and Legendre polynomials, are all susceptible to internal discontinuity (Gottlieb and Orszag (1977)). The eigenfunctions determined here through a mode matching technique have a global support and hence Gibbs overshoots arise below the surface layer particularly within the pycnocline. We note that the presence of high level background turbulence activity of tidal origin at the bottom layer is helpful in suppressing the Gibbs phenomenon.

In follow-up researches the Galerkin spectral method will be used mainly to gain physical insight into stratified flows whenever a well-formed layered system can be assumed and the vertical structure of eddy viscosity is fixed.

REFERENCES

Canuto, C., 1987. Topics in spectral methods for hyperbolic equations In: Partial differential equations of hyperbolic type and applications, G. Geymonat (editor), 1-32, World Scientific Publishing Co., Singarpore.

Davies, A.M., 1983. Application of a Galerkin-Eigenfunction method to computing currents in homogeneous and stratified seas, In: Numerical Methods for Fluid Dynamics, K.W. Morton and M.J. Bains (editors), 287-301, Academic Press.

Davies, A.M., 1985a. A three-dimensional modal model of wind induced flow in a sea region, *Prog. Oceanogr.*, **15:** 71-128.

Davies, A.M., 1985b. Application of a sigma coordinate sea model to the calculation of wind induced currents. *Cont. Shelf Res.;* **4:** 389-423.

Davies, A.M., 1986. Application of a spectral model to the calculation of wind drift currents in an idealised stratified sea, *Cont. Shelf Res.*, **5:** 579-610.

Davies, A.M. and Furnes, G.K., 1986. On the determination of vertical structure functions for time-dependent flow problems, *Tellus*, **38a:** 462-477.

Davies, A.M. and Owen, A., 1979. Three-dimensional numerical sea model using the Galerkin method with a polynomial basis set, *Appl. Math. Modelling*, **3**, 421-428.

Furnes, G.K., 1983. A three-dimensional numerical sea model with eddy viscosity varying piecewise linearly in the vertical, *Cont. Shelf Res.*, **2:** 231-241.

Gottlieb, D. and S.A. Orszag, 1977. Numerical analysis of spectral methods: theory and application, NSF-CBMS Monogr., 26, *Soc. Ind. and Appl. Math. Philadelphia.*

Heaps, N.S., 1983. Development of a three-layered spectral model for the motion of a stratified shelf sea. I. Basic equations, In: Physical Oceanography of Coastal and Self Seas, B. Johns (editor), 387-400, Elsevier.

Heaps, N.S. and Jones, J.E., 1983. Development of a three-layered spectral model for the motion of a stratified shelf sea. II. Experiments with a rectangular basin representing the Celtic Sea, *In:* Physical Oceanography of Coastal and Shelf Seas. B. Johns (editor), 401-465, Elsevier

Heaps, N.S. and Jones, J.E., 1985. A three-layered spectral model with application to wind induced motion in the presence of stratification and a bottom slope, *Cont. Shelf Res.*, **4**, 279-319.

Jung, K. and Noye, J., 1988. A spectral method of determining depth variations of currents in a two-layer stratified sea, *In:* Computational Techniques and Applications: CTAC 87, J. Noye (editor), 333-346, North-Holland.

Jung, K., 1989. On three-dimensional hydrodynamic numerical modelling of wind induced flows in stably stratified waters: a Galerkin-Finite difference approach, Ph. D. thesis, The Univ. of Adelaide.